



Supplement of

Co-registration and residual correction of digital elevation models: a comparative study

Tao Li et al.

Correspondence to: Xiang Shen (shen@apm.ac.cn)

The copyright of individual parts of the supplement might differ from the article licence.

Contents of this file

Greenland Ice Sheet (GrIS) case study

High Mountain Asia (HMA) case study

5 New Zealand (NZL) case study

The method of NH

Abbreviations

NK: the method of Nuth and Kääb

RT: the method of Rosenholm and Torlegard

10 NH: the method of Noh and Howat

1. GrIS case study

Table S1. Co-registration results of the 23 DEM pairs in GrIS. The MedAD values of the RT method are presented and compared with the linear version of the NK method.

Pair ID	DEM	Roles	Date	Resolution (m)	Scene ID	MedAD (Reduced)
GrIS-1	ASTER	Reference	5 Aug 2014	30	AST14DEM.003:2133338256	6.140 (11.8%)
	ASTER	Secondary	7 Aug 2003	30	AST14DEM.003:2015893657	
GrIS-2	ASTER	Reference	25 Jul 2016	30	AST14DEM.003:2237110490	5.916 (0.4%)
	ASTER	Secondary	17 Jun 2002	30	AST14DEM.003:2007321075	
GrIS-3	ASTER	Reference	21 Aug 2020	30	AST14DEM.003:2396978128	6.176 (9.8%)
	ASTER	Secondary	16 Jun 2019	30	AST14DEM.003:2341532177	
GrIS-4	ASTER	Reference	25 Jul 2016	30	AST14DEM.003:2237110490	5.580 (1.7%)
	ASTER	Secondary	11 Jul 2005	30	AST14DEM.003:2030001029	
GrIS-5	ASTER	Reference	5 Aug 2003	30	AST14DEM.003:2015777895	6.749 (5.3%)
	ASTER	Secondary	26 Jun 2006	30	AST14DEM.003:2034745465	
GrIS-6	ASTER	Reference	6 Jun 2007	30	AST14DEM.003:2043591221	12.289 (1.2%)
	ASTER	Secondary	21 Jul 2012	30	AST14DEM.003:2119138452	
GrIS-7	ASTER	Reference	17 Jun 2002	30	AST14DEM.003:2007321076	6.827 (8.6%)
	ASTER	Secondary	11 Jul 2005	30	AST14DEM.003:2030001032	
GrIS-8	ASTER	Reference	17 Jun 2002	30	AST14DEM.003:2007321076	5.301 (0.9%)
	ASTER	Secondary	25 Jul 2016	30	AST14DEM.003:2237110508	
GrIS-9	ASTER	Reference	17 Jun 2002	30	AST14DEM.003:2007321076	5.612 (0.1%)
	ASTER	Secondary	6 Jul 2003	30	AST14DEM.003:2015233147	
GrIS-10	ASTER	Reference	17 Jun 2002	30	AST14DEM.003:2007321076	5.423 (2.9%)
	ASTER	Secondary	22 Jun 2004	30	AST14DEM.003:2024616433	
GrIS-11	ASTER	Reference	5 Aug 2003	30	AST14DEM.003:2015777888	7.900 (15.3%)
	ASTER	Secondary	26 Jun 2006	30	AST14DEM.003:2034745466	
GrIS-12	ASTER	Reference	5 Jul 2006	30	AST14DEM.003:2034888289	8.794 (0.3%)
	ASTER	Secondary	17 Aug 2016	30	AST14DEM.003:2240132072	
GrIS-13	ASTER	Reference	5 Jul 2006	30	AST14DEM.003:2034888289	6.687 (0.7%)
	ASTER	Secondary	11 Jul 2014	30	AST14DEM.003:2132976700	
GrIS-14	ASTER	Reference	5 Jul 2006	30	AST14DEM.003:2034888289	5.132 (2.0%)
	ASTER	Secondary	21 Jul 2006	30	AST14DEM.003:2035293364	
GrIS-15	ASTER	Reference	26 Jul 2017	30	AST14DEM.003:2267749658	5.641 (0.4%)
	ASTER	Secondary	1 Aug 2019	30	AST14DEM.003:2345264318	
GrIS-16	ASTER	Reference	26 Jul 2017	30	AST14DEM.003:2267749658	7.436 (2.7%)
	ASTER	Secondary	19 Aug 2020	30	AST14DEM.003:2396408309	
GrIS-17	ASTER	Reference	19 Aug 2020	30	AST14DEM.003:2396408312	6.795 (4.0%)
	ASTER	Secondary	1 Aug 2019	30	AST14DEM.003:2345264317	
GrIS-18	ASTER	Reference	19 Aug 2020	30	AST14DEM.003:2396408312	5.903 (5.9%)
	ASTER	Secondary	26 Jul 2017	30	AST14DEM.003:2267749652	
GrIS-19	ASTER	Reference	19 Aug 2020	30	AST14DEM.003:2396408317	5.895 (9.2%)
	ASTER	Secondary	1 Aug 2019	30	AST14DEM.003:2345264332	
GrIS-20	ASTER	Reference	8 Aug 2016	30	AST14DEM.003:2238723197	7.561 (1.1%)
	ASTER	Secondary	2 Aug 2008	30	AST14DEM.003:2066350356	
GrIS-21	ASTER	Reference	8 Aug 2016	30	AST14DEM.003:2238723197	8.524 (1.8%)
	ASTER	Secondary	2 Jul 2020	30	AST14DEM.003:2384667768	
GrIS-22	ASTER	Reference	17 Jun 2002	30	AST14DEM.003:2007321076	5.620 (0.2%)
	ASTER	Secondary	6 Jul 2003	30	AST14DEM.003:2015233147	
GrIS-23	ASTER	Reference	17 Jun 2002	30	AST14DEM.003:2007321076	9.403 (11.8%)

15 **2. HMA case study**

Table S2. Co-registration results of the 22 DEM pairs in HMA. The MedAD values of the RT method are presented and compared with the linear version of the NK method.

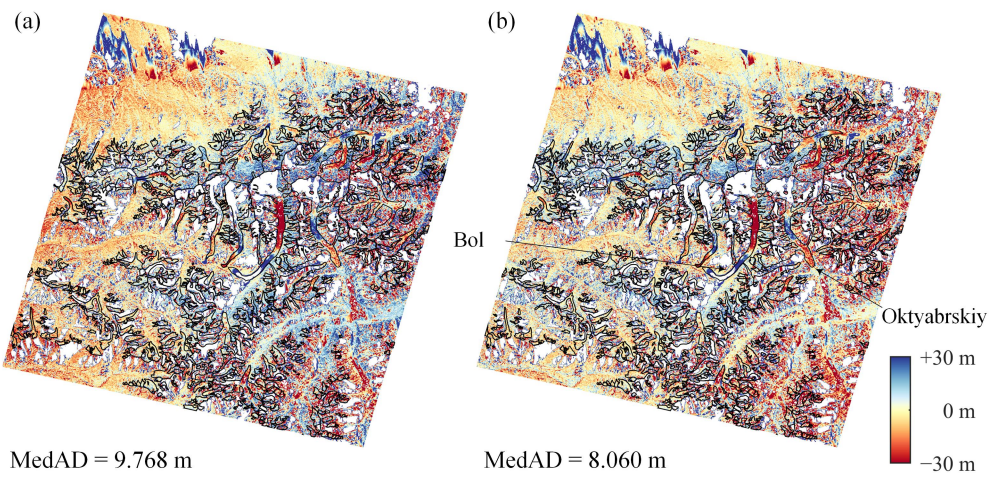
Pair ID	DEM	Roles	Date	Resolu-tion (m)	Scene ID	MedAD (Reduced)
HMA-1	Copernicus	Reference	2011–2015	30	N37E073, N38E073	0.780 (83.3%)
	ZY-3	Secondary	8 Oct 2017	30	—	
HMA-2	ASTER	Reference	22 Aug 2005	30	AST14DEM.003:2030590191	7.561 (11.2%)
	ASTER	Secondary	7 Sept 2005	30	AST14DEM.003:2030819798	
HMA-3	SRTM	Reference	11–22 Feb 2000	30	N39E073	6.366 (26.0%)
	ASTER	Secondary	22 Aug 2005	30	AST14DEM.003:2030590191	
HMA-4	SRTM	Reference	11–22 Feb 2000	30	N39E073	5.790 (8.6%)
	ASTER	Secondary	7 Sept 2005	30	AST14DEM.003:2030819798	
HMA-5	SRTM	Reference	11–22 Feb 2000	30	N39E072, N39E073, N38E072, N38E073	8.060 (17.5%)
	ASTER	Secondary	22 Mar 2005	30	AST14DEM.003:2028219582	
HMA-6	ZY-3	Reference	8 Oct 2017	30	—	5.063 (17.4%)
	ASTER	Secondary	10 Oct 2017	30	AST14DEM.003:2280543414	
HMA-7	ASTER	Reference	10 Oct 2017	30	AST14DEM.003:2280543414	6.621 (8.3%)
	ASTER	Secondary	26 Oct 2017	30	AST14DEM.003:2281248034	
HMA-8	ZY-3	Reference	8 Oct 2017	30	—	8.468 (19.3%)
	ASTER	Secondary	26 Oct 2017	30	AST14DEM.003:2281248034	
HMA-9	ZY-3	Reference	8 Oct 2017	30	—	9.004 (13.5%)
	ASTER	Secondary	3 Oct 2017	30	AST14DEM.003:2280252518	
HMA-10	Copernicus	Reference	2011–2015	30	N36E071	1.429 (42.3%)
	ZY-3	Secondary	2 Dec 2016	30	—	
HMA-11	Copernicus	Reference	2011–2015	30	N38E072, N38E073	2.296 (31.9%)
	ZY-3	Secondary	28 Sept 2017	30	—	
HMA-12	Copernicus	Reference	2011–2015	30	N38E074, N38E075	1.081 (31.5%)
	ZY-3	Secondary	31 Dec 2017	30	—	
HMA-13	ASTER	Reference	25 Sept 2020	30	AST14DEM.003:2406369987	9.954 (9.6%)
	ASTER	Secondary	27 Oct 2020	30	AST14DEM.003:2421038656	
HMA-14	ASTER	Reference	21 Sept 2021	30	AST14DEM.003:2487838647	6.818 (20.0%)
	ASTER	Secondary	6 Jul 2022	30	AST14DEM.003:2555146603	
HMA-15	ASTER	Reference	30 Jul 2020	30	AST14DEM.003:2391299920	11.613 (0.2%)
	ASTER	Secondary	8 Oct 2022	30	AST14DEM.003:2566467729	
HMA-16	Copernicus	Reference	2011–2015	30	N38E074, N38E075	6.975 (6.0%)
	ASTER	Secondary	9 Sept 2020	30	AST14DEM.003:2401419492	
HMA-17	Copernicus	Reference	2011–2015	30	N38E072	8.395 (5.6%)
	ASTER	Secondary	27 Jul 2022	30	AST14DEM.003:2556749721	
HMA-18	ASTER	Reference	4 Jul 2022	30	AST14DEM.003:2554781302	5.162 (2.4%)
	ASTER	Secondary	5 Aug 2022	30	AST14DEM.003:2557726160	
HMA-19	SRTM	Reference	11–22 Feb 2000	30	N37E071	4.246 (0.7%)
	ZY-3	Secondary	17 Sept 2018	30	—	
HMA-20	SRTM	Reference	11–22 Feb 2000	30	N37E070, N38E070	6.605 (5.9%)
	ZY-3	Secondary	30 Jun 2018	30	—	
HMA-21	SRTM	Reference	11–22 Feb 2000	30	N37E070, N38E070, N37E071	6.238 (2.0%)

	ZY-3	Secondary	19 Sept 2016	30	—	
HMA-22	SRTM	Reference	11–22 Feb 2000	30	N37E071, N38E071	8.541 (3.3%)
	ZY-3	Secondary	7 Sept 2018	30	—	

Some representative results are demonstrated below. Since the three versions of the NK method always produce similar
20 co-registration results, we only compare the linear version of the NK method with the RT method to make figures clear.

1) Large fraction of glacier areas vs. stable terrain.

The DEM pair HMA-5 is located in the northern Pamirs, covered by a great number of mountain glaciers. We removed the saturated pixels over bright snow-covered areas (e.g., upstream of Bol and Oktyabrskiy glaciers). It can be seen from Fig. S1 that the RT method effectively eliminates the residuals in the east-west direction of the NK results.

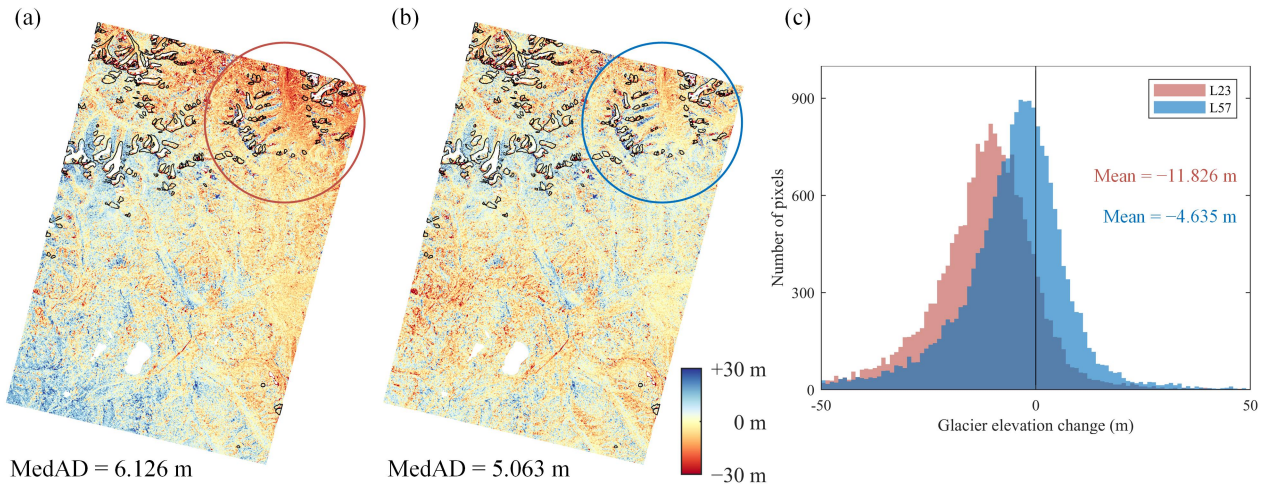


25

Figure S1. Co-registration results of the HMA-5 DEM pair. The NK method (a) and the RT method (b). The black lines mark the RGI 6.0 glacier outlines.

2) Reference DEM and secondary DEM are measured at a very short time interval

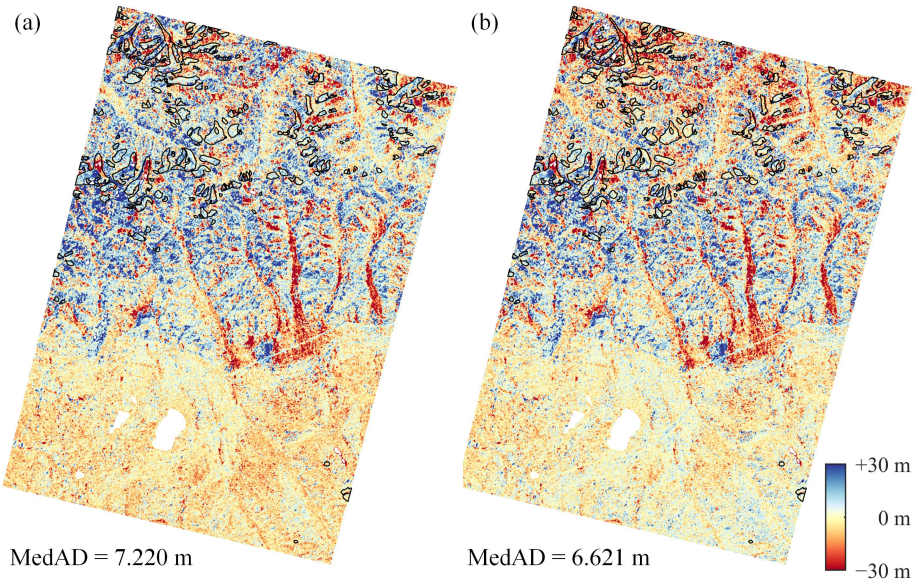
In addition to the ASTER DEM pair HMA-3 in the manuscript, HMA-6 is also used for validating the co-registration
30 results over ice-covered terrain. The DEM pair consists of ZY-3 DEM 20171008 and ASTER DEM 20171010, which are measured two days apart. The co-registration results of the NK method show systematic errors in the southwest-northeast direction, resulting in a significantly negative bias (-11.826 m) in the northeast region (within the red circle in Fig. S2a). In contrast, the glacier elevation changes estimated by the RT method are much closer to zero.



35 **Figure S2.** Co-registration results of the HMA-6 DEM pair. The NK method (a) and the RT method (b). The black lines mark the RGI 6.0 glacier outlines. The histogram of elevation change for glaciers within the circle (c).

3) The rough topography leads to a high noise level in the DEMs

Figure S3 depicts the co-registration results of the DEM pair HMA-7 with a high noise level. The co-registration error of the RT method is 8.3% smaller than that of the NK method.



40 **Figure S3.** Co-registration results of the HMA-7 DEM pair. The NK method (a) and the RT method (b). The black lines mark the RGI 6.0 glacier outlines.

4) Significant attitude errors

As shown in Fig. S4, the ZY-3 DEM 20161202 of HMA-10 suffers from significant attitude errors. The RT method 45 effectively eliminates the residual trend in the northwest-southeast direction of the NK results.

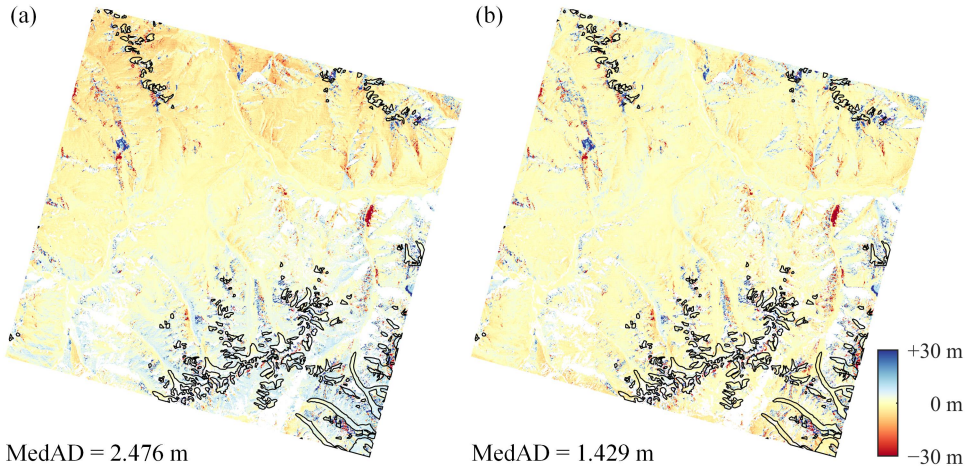


Figure S4. Co-registration results of the HMA-10 DEM pair. The NK method (a) and the RT method (b). The black lines mark the RGI 6.0 glacier outlines.

3. NZL case study

As shown in Fig. S5, we selected 11 DEM pairs (listed in Table S3) in the Southern Alps region of NZL for DEM co-registration experiments.

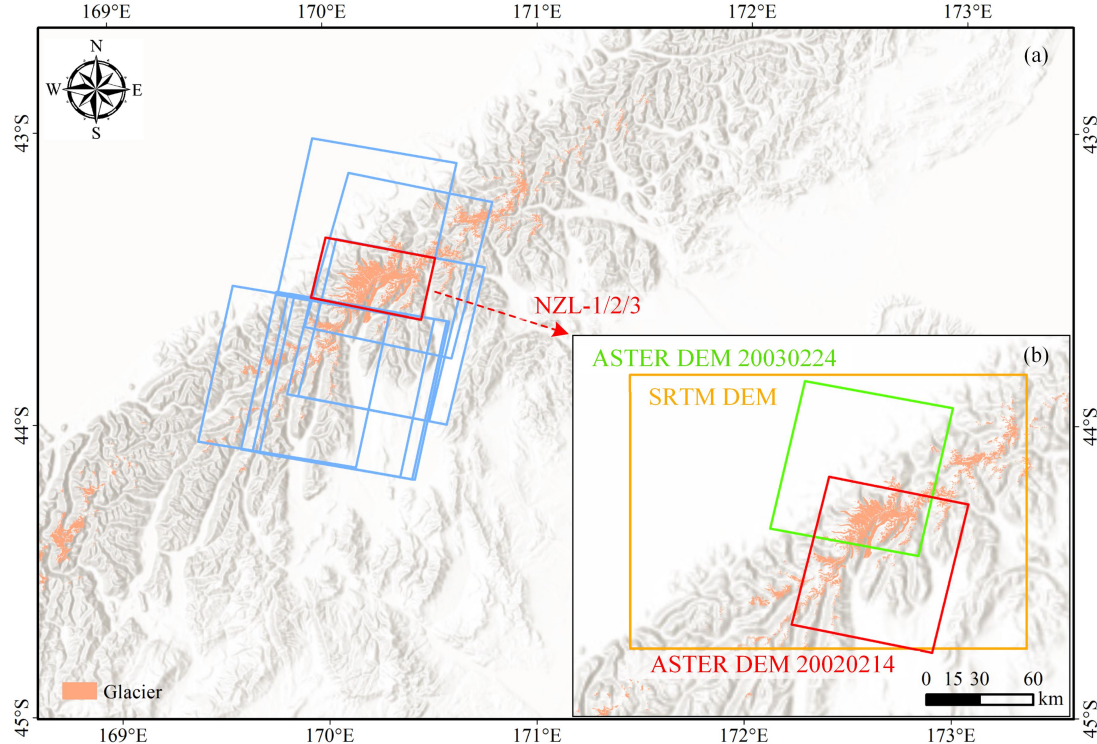


Figure S5. The study area located on NZL. (a) The footprints (blue) of the 11 DEM pairs, DEM pairs NZL-1/2/3 are highlighted in red. (b) The coverage of the three DEM images in NZL-1/2/3 (orange: SRTM DEM; red: ASTER DEM 20020214; green: ASTER DEM 20030224). The glacierized areas are from the RGI 6.0 inventory.

55

Table S3. Co-registration results of the 11 DEM pairs in NZL. The MedAD values of the RT method are presented and compared with the linear version of the NK method.

Pair ID	DEM	Roles	Date	Resolu-tion (m)	Scene ID	MedAD (Reduced)
NZL-1	SRTM	Reference	11–22 Feb 2000	30	S44E169, S44E170	5.627 (4.5%)
	ASTER	Secondary	14 Feb 2002	30	AST14DEM.003:2013763401	
NZL-2	ASTER	Reference	14 Feb 2002	30	AST14DEM.003:2013763401	5.966 (9.0%)
	ASTER	Secondary	24 Feb 2003	30	AST14DEM.003:2011883607	
NZL-3	SRTM	Reference	11–22 Feb 2000	30	S44E169, S44E170	6.871 (13.0%)
	ASTER	Secondary	24 Feb 2003	30	AST14DEM.003:2011883607	
NZL-4	SRTM	Reference	11–22 Feb 2000	30	S44E169, S44E170	6.136 (5.8%)
	ASTER	Secondary	9 Feb 2006	30	AST14DEM.003:2033045873	
NZL-5	SRTM	Reference	11–22 Feb 2000	30	S44E169, S44E170	6.278 (13.9%)
	ASTER	Secondary	24 Feb 2003	30	AST14DEM.003:2011883607	
NZL-6	ASTER	Reference	13 Mar 2021	30	AST14DEM.003:2438508389	9.002 (1.5%)
	ASTER	Secondary	1 Apr 2022	30	AST14DEM.003:2543057148	
NZL-7	SRTM	Reference	11–22 Feb 2000	30	S44E169, S44E170, S45E169, S45E170	9.435 (10.0%)
	ASTER	Secondary	30 Apr 2021	30	AST14DEM.003:2450214224	
NZL-8	SRTM	Reference	11–22 Feb 2000	30	S44E169, S44E170, S45E169, S45E170	6.491 (8.6%)
	ASTER	Secondary	8 Mar 2019	30	AST14DEM.003:2331203149	
NZL-9	SRTM	Reference	11–22 Feb 2000	30	S44E169, S44E170, S45E169, S45E170	9.214 (15.7%)
	ASTER	Secondary	24 May 2018	30	AST14DEM.003:2295763239	
NZL-10	SRTM	Reference	11–22 Feb 2000	30	S44E169, S44E170, S45E169, S45E170	16.626 (0.4%)
	ASTER	Secondary	28 May 2022	30	AST14DEM.003:2549984322	
NZL-11	SRTM	Reference	11–22 Feb 2000	30	S44E169, S44E170, S45E169, S45E170	6.651 (1.0%)
	ASTER	Secondary	9 Feb 2020	30	AST14DEM.003:2359064856	

Table S4 shows the co-registration results for the 11 DEM pairs of NZL. The RT method reduces up to 15.7% more co-
60 registration errors compared to the NK method.

Table S4. Co-registration results obtained with the 11 DEM pairs of NZL.

Method	Average MedAD (m)
Before co-registration	13.727
NK standard version	8.656
NK simplified version	8.657
NK linear version	8.656
RT	8.027

As shown in Fig. S6c, the DEM pair NZL-3 contains a large number of unstable pixels (forest land, water, wetland, and glacier and snow cover) on the west side of the image. The co-registration results in Fig. S6 a and b demonstrate that the RT
65 method reduces the error trend in the east-west direction of the NK results.

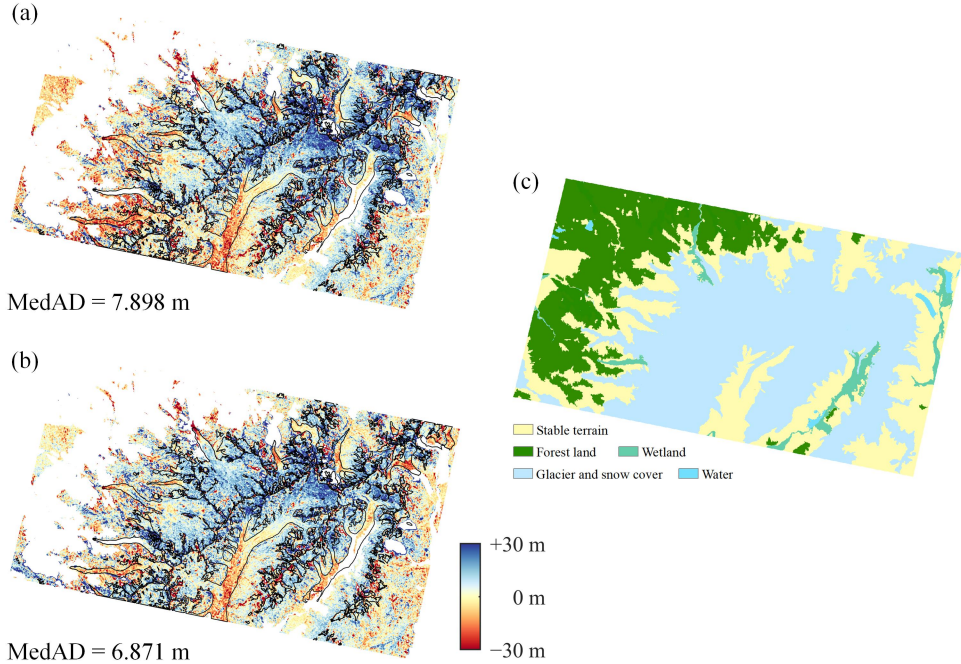


Figure S6. Co-registration results of the NZL-3 DEM pair. The NK method (a) and the RT method (b). The black lines mark the RGI 6.0 glacier boundaries. The land cover map from the GlobeLand30 product (c).

4. The method of NH

70 In the DEM co-registration method of NH (Noh and Howat, 2014), the coordinate update equation is given by

$$\begin{bmatrix} X \\ Y \\ Z \end{bmatrix}_i = \begin{bmatrix} \Delta X \\ \Delta Y \\ \Delta Z \end{bmatrix} + sR_\omega R_\varphi R_\kappa \begin{bmatrix} X \\ Y \\ Z \end{bmatrix}_{i-1} \quad (\text{S1})$$

where R_ω , R_φ and R_κ are three rotation matrices derived from Euler angles.

$$R_\omega = \begin{pmatrix} 1 & 0 & 0 \\ 0 & \cos(\omega) & -\sin(\omega) \\ 0 & \sin(\omega) & \cos(\omega) \end{pmatrix}$$

$$R_\varphi = \begin{pmatrix} \cos(\varphi) & 0 & \sin(\varphi) \\ 0 & 1 & 0 \\ -\sin(\varphi) & 0 & \cos(\varphi) \end{pmatrix} \quad (\text{S2})$$

$$R_\kappa = \begin{pmatrix} \cos(\kappa) & -\sin(\kappa) & 0 \\ \sin(\kappa) & \cos(\kappa) & 0 \\ 0 & 0 & 1 \end{pmatrix}$$

The partial derivative of Eq. (S1) with respect to seven parameters (three translation parameters, one scale factor, and

75 three Euler angles) is written as

$$\begin{bmatrix} dX \\ dY \\ dZ \end{bmatrix} = \begin{bmatrix} d\Delta X \\ d\Delta Y \\ d\Delta Z \end{bmatrix} + \begin{bmatrix} C_{11} \\ C_{21} \\ C_{31} \end{bmatrix} ds + \begin{bmatrix} C_{12} & C_{13} & C_{14} \\ C_{22} & C_{23} & C_{24} \\ C_{32} & C_{33} & C_{34} \end{bmatrix} \begin{bmatrix} d\omega \\ d\varphi \\ d\kappa \end{bmatrix} \quad (\text{S3})$$

where

$$\begin{aligned} C_{11} &= Z \sin(\varphi) + X \cos(\kappa) \cos(\varphi) - Y \cos(\varphi) \sin(\kappa) \\ C_{12} &= 0 \\ C_{13} &= sZ \cos(\varphi) + sY \sin(\kappa) \sin(\varphi) - sX \cos(\kappa) \sin(\varphi) \\ C_{14} &= -sY \cos(\kappa) \cos(\varphi) - sX \cos(\varphi) \sin(\kappa) \\ C_{21} &= X(\cos(\omega) \sin(\kappa) + \cos(\kappa) \sin(\omega) \sin(\varphi)) + Y(\cos(\kappa) \cos(\omega) - \sin(\kappa) \sin(\omega) \sin(\varphi)) - Z \cos(\varphi) \sin(\omega) \\ C_{22} &= -sX(\sin(\kappa) \sin(\omega) - \cos(\kappa) \cos(\omega) \sin(\varphi)) - sY(\cos(\kappa) \sin(\omega) + \cos(\omega) \sin(\kappa) \sin(\varphi)) - sZ \cos(\omega) \cos(\varphi) \\ C_{23} &= sZ \sin(\omega) \sin(\varphi) + sX \cos(\kappa) \cos(\varphi) \sin(\omega) - sY \cos(\varphi) \sin(\kappa) \sin(\omega) \\ C_{24} &= sX(\cos(\kappa) \cos(\omega) - \sin(\kappa) \sin(\omega) \sin(\varphi)) - sY(\cos(\omega) \sin(\kappa) + \cos(\kappa) \sin(\omega) \sin(\varphi)) \\ C_{31} &= X(\sin(\kappa) \sin(\omega) - \cos(\kappa) \cos(\omega) \sin(\varphi)) + Y(\cos(\kappa) \sin(\omega) + \cos(\omega) \sin(\kappa) \sin(\varphi)) + Z \cos(\omega) \cos(\varphi) \\ C_{32} &= sX(\cos(\omega) \sin(\kappa) + \cos(\kappa) \sin(\omega) \sin(\varphi)) + sY(\cos(\kappa) \cos(\omega) - \sin(\kappa) \sin(\omega) \sin(\varphi)) - sZ \cos(\varphi) \sin(\omega) \\ C_{33} &= sY \cos(\omega) \cos(\varphi) \sin(\kappa) - sX \cos(\kappa) \cos(\omega) \cos(\varphi) - sZ \cos(\omega) \sin(\varphi) \\ C_{34} &= sX(\cos(\kappa) \sin(\omega) + \cos(\omega) \sin(\kappa) \sin(\varphi)) - sY(\sin(\kappa) \sin(\omega) - \cos(\kappa) \cos(\omega) \sin(\varphi)) \end{aligned} \quad (\text{S4})$$

The above equations are Eqs. (19–21) in Noh and Howat (2014). Considering that the Euler angles are nearly equal to

80 zero in DEM co-registration tasks, Eq. (S3) can be approximated by

$$\begin{bmatrix} dX \\ dY \\ dZ \end{bmatrix} \approx \begin{bmatrix} d\Delta X \\ d\Delta Y \\ d\Delta Z \end{bmatrix} + \begin{bmatrix} X \\ Y \\ Z \end{bmatrix} ds + s \begin{bmatrix} 0 & Z & -Y \\ -Z & 0 & X \\ Y & -X & 0 \end{bmatrix} \begin{bmatrix} d\omega \\ d\varphi \\ d\kappa \end{bmatrix} \quad (\text{S5})$$

It can be seen that Eq. (S5) is equivalent to the Eq. (11) used in the method of Rosenholm and Torlegard.

References:

- 85 Noh, M. and Howat, I. M.: Automated Coregistration of Repeat Digital Elevation Models for Surface Elevation Change Measurement Using Geometric Constraints, IEEE Trans. Geosci. Remote Sensing, 52, 2247–2260, <https://doi.org/10.1109/TGRS.2013.2258928>, 2014.